MR댐퍼를 이용한 지진하중을 받는 지진격리 벤치마크 구조물의 신경망제어

Neuro-Control of Seismically Excited Base-Isolated Benchmark Structure using MR Damper

이헌재*1) 조상원** 오주원*** 이인원****
Lee, Heon Jae Cho, Sang Won Oh, Ju Won Lee, In Won

ABSTRACT

이 논문에서는 신경망 제어기와 MR 댐퍼를 이용하여 지진하중을 받는 지진격리 벤치마크 구조물의 응답 감소를 위한 반능동 제어방법이 제안되었다. 제안방법 중 신경망 제어기에는 적절한 제어력을 산출하기 위해 가격함수를 기반으로한 학습 알고리즘과 간편한 민감도 계산기법이 도입되었다. MR 댐퍼가 계산되어진 제어력과 비슷한 제어력을 낼 수 있도록 clipped 알고리즘을 이용하였고, 제안된 반능동 신경망 제어방법이 지진격리 장치가 설치된 벤치마크 구조물에 적용되었다. 수치해석에서는 벤치마크 문제를 정의한 논문에서 제공된 수동제어방법이나 예시제어방법과 제안방법의 제어성능을 비교하였다. 수치해석 결과 제안방법은 지하 변위를 약간 증가시키지만, 각층의 가속도, base shear, building corner drift 등을 매우 효과적으로 줄이는 것으로 판명되었다.

1. Introduction

One of the most widely implemented and accepted seismic protection systems is base isolation. Seismic base isolation (Skinner et al. 1993; Naeim and Kelly 1999) is a technique that mitigates the effects of an earthquake by essentially isolating the structure and its contents from potentially dangerous ground motion, especially in the frequency range where the building is most affected.

In base isolation systems, nonlinear devices such as lead-rubber bearings, friction pendulum bearings, or high damping rubber bearings are often used. The benefit of these types of bearings is that the restoring force and adequate damping capacity can be obtained in one device. However, because the dynamic characteristics of these devices are strongly nonlinear, the vibration reduction is not optimal for a wide range of input ground motion intensities, especially those strong impulsive ground motions generated at near-source locations (Hall et al. 1995; Heaton et al. 1995).

Seeking to develop isolation systems that can be effective for a wide range of ground excitations, hybrid control strategies, consisting of a passive isolation system combined with actively controlled actuators, have been investigated by a number of

*한국과학기술원 건설및환경공학과, 박사과정, **University of Western Ontario, Canada, 박사후연수과정
***한남대학교 토목환경공학과, 교수, **정회원·한국과학기술원 건설및환경공학과, 명예교수

researchers (e.g., Kelly et al. 1987; Inaudi and Kelly 1990; Nagarajaiah et al. 1993; Yang et al. 1996; Nishimura and Kojima 1998). One of the hybrid base isolation systems employs semiactive control devices, such as magnetorheological (MR) dampers (Spencer et al. 1997; Yang et al. 2002, 2004). Semiactive systems have gained significant attentions in recent years because these systems have the capability of adapting to changes in external loading conditions, similar to the active protective system, but without requiring access to large power supplies. Some researchers have applied these devices both analytically and experimentally to develop semiactive base isolation systems (Johnson et al. 1999; Ramallo et al. 2000a,b; Yang and Agrawal 2001). Saharabudhe et al. (2005) experimentally showed the effectiveness of semiactive base isolation for a single span bridge model using MR dampers.

In this paper, an improved semi-active nerual network-based controller (Kim and Lee 2001, Lee et al. 2003) in conjunction with MR dampers is employed in vibration reduction of a base-isolated benchmark structure proposed by Narasimhan et al. (2005). In the proposed neuro-controller, which was developed by employing a new training algorithm based on a cost function and a sensitivity evaluation algorithm to replace an emulator neural network, produces the desired control force, and then a clipped algorithm clips the control force that cannot be achieved by an MR damper. Numerical simulation results are compared with passive and sampler controller results provided by Nagarajaiah and Narasimhan (2005) and show that the proposed semi-active neurocontroller is effective in reducing the vibration of the base-isolated benchmark structure.

2. Benchmark Structure

The benchmark structure is a base-isolated eight-story, steel-braced framed building, 82.4-m long and 54.3-m wide, similar to existing buildings in Los Angeles, California. The superstructure and the base are modeled using three master degrees of freedom (DOF) per floor at the center of mass. The combined model of the superstructure (24 DOFs) and isolation system (3 DOFs) consists of 27 degrees of freedom. The nominal isolation system consists of both friction pendulu bearings and linear elastometric bearings. However, in this paper, we only considered the linear elastomeric isolation system which consists of 92 bearings installed between the structural base and foundation. In addition, total of 16 MR dampers (8 along the x-axis and 8 along the y-axis) are also installed with the isolation system for semi-active vibration control of the structure. For details on mathematical modeling of the benchmark structure, interesting readers can refer to the paper written by Narasimhan et al. (2005).

3. Semiactive Neuro-Controller

The neural network approach for structural vibration control was first proposed by Ghaboussi and Joghataie (1995) and Chen et al. (1995). They used the so-called emulator neural network for the identification of the structural system and trained controller neural network by means of the emulator neural network. Another training method was proposed by Kim and Lee (2001) using a kind of cost function. Therefore, one does not have to

preset the desired structural response to train a neural network. In addition, Kim and Lee also proposed an off-line sensitivity evaluation scheme to replace the emulator neural network which is used on-line to predict structural response sensitivity. As a result, the required effort to train the emulator neural network can be eliminated.

To applythe neuro-control algorithm to semi-active devices (e.g. MR dampers), Lee et al. (2003) proposed a semi-active neuro-control system. The block diagram is shown in Figure 1. The control system, in addition to the neuro-controller, consists of a clipped algorithm. In this approach, the neuro-controller first calculates the optimal control force. To induce the MR damper to generate approximately the desired optimal control force, a clipped algorithm (Dyke et al. 1996) is then employed to select the input voltage to the MR damper, which is defined as

$$v = V_{\max} H\{(f_d - f)f\} \tag{1}$$

where $V_{\max}$ is the voltage to the current driver associated with saturation of the magnetic field in the MR damper, and $H(\cdot)$ is the Heaviside step function. For the clipped algorithm, when the MR damper is providing the desired optimal force (i.e., $f = f_d$), the voltage applied to the damper should remain at the present level. If the magnitude of the force produced by the damper is smaller than the magnitude of the desired optimal force and the two forces have the same sign, the voltage applied to the current driver is increased to the maximum level so as to increase the force produced by the damper to match the desired control force. Otherwise, the commanded voltage is set to zero. This control algorithm has the benefit that a model of the damper is not required in the control design, although the model is important for system analysis.

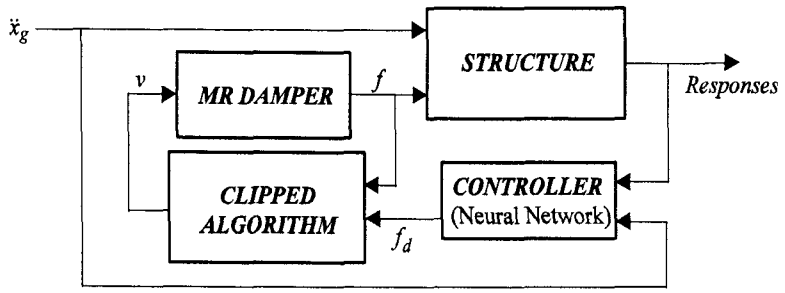

Fig. 1. Block diagram of semi-active neuro-control system using MR damper

4. Neuro-Controller Training Algorithm

The training of nerual work is based on the minimization of a cost function. The cost function defined in discrete-time domain is expressed by

$$\hat{J} = \frac{1}{2}\sum_{k=0}^{N_f-1}\left\{y_{k+1}^T Q y_{k+1} + u_k^T R u_k\right\} = \frac{1}{2}\sum_{k=0}^{N_f-1}\hat{J}_k \tag{2}$$

where $y(n\times 1)$ and $u(m\times 1)$ are specific states and control signals; $Q(n\times n)$ and $R(m\times m)$ are weighting matrices; k and N_f are sampling number and total number of sampling time. Each term in braces of Eq. (2) is non-dimensionalized by weighting matrices Q and R.

The update of weights ΔW_{ji}^2 and biases Δb_j^2 between the output layer and hidden layer can be simply expressed as

$$\Delta W_{ji}^2 = \psi^2 \{o_i^1\}^T \tag{3}$$

$$\Delta b_j^2 = \psi^2 \tag{4}$$

where

$$\psi^2 = -\eta \left(y_{k+1}^T Q \left\{ \frac{\partial y_{k+1}}{\partial u_k} \right\} + u_k^T R \{1\} \right) \left(f^2 \right)' \tag{5}$$

and η, $\partial y_{k+1}/\partial u_k$, $\{1\}$, f^2 are learning rate, sensitivity, $m \times 1$ unit vector and activation function of the output layer, respectively. By varying the learning rate η, the convergence of training can be improved. However, if the learning rate is too large, training may become unstable.

In the same manner, update of weights ΔW_{ih}^1 and biases Δb_i^1 between hidden layer and input layer can be obtained by

$$\Delta W_{ih}^1 = \psi^1 \{I_h\}^T \tag{6}$$

$$\Delta b_i^1 = \psi^1 \tag{7}$$

and

$$\psi^1 = \left\{ \{W_{ji}^2\}^T \psi^2 \right\} \cdot \left(f^1 \right)' \tag{8}$$

where • is the net product.

In updating the weights and biases of neural network, there are many coefficients need to be selected by experience or trial and error. Learning rate, training acceleration factors, ending condition, and weighting matrices for cost function should be appropriately selected so that the results of updating converge. If cost function during an epoch decreases compared with that of previous epoch, a larger learning rate η will be used to accelerate the training of neural network. In contrast, if the cost function increases, a smaller learning rate will be utilized to improve the training procedure. The rates of increasing or decreasing learning rate are called training acceleration factors. When the learning rate becomes very small, the training will be stopped as the cost function converges.

Because feedback signals to the neural network is relatively large in this specific benchmark problem, the learning rate should be small enough, which was chosen as 5×10^{-7}. For training acceleration factor, 1.05 and 0.1 are employed, respectively. Training is repeated until the number of epochs reaches 100 or the learning rate is less than 1×10^{-10}. Figure 2 shows the cost function versus epochs for the proposed semi-active neuro-controller. As can be seen, the cost functionconverges in both x and y-directions of the benchmark structure, which means the training is successful.

An artificial filtered earthquake record (shown in Fig. 3) was employed to train the neuro-controller. The magnitude of this earthquake record was scaled to match the maximum acceleration (8.58 m/sec2) of the Sylmar earthquake FN component. The shaping filter employed is as follows (Nagarajaiah and Narasimhan 2005)

$$F(s) = \frac{4\zeta_g \omega_g s}{s^2 + 2\zeta_g \omega_g s + \omega_g^2} \tag{9}$$

where $\omega_g = 2\pi$ rad/sec, $\zeta_g = 0.3$.

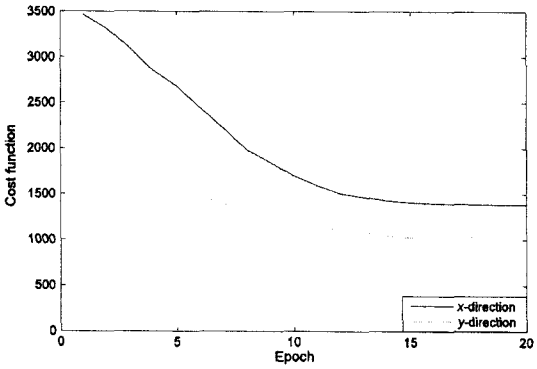

Fig. 2. Cost function vs. epoch in both x and y-directions

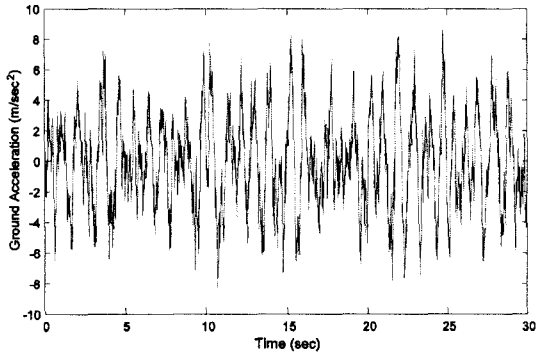

Fig. 3. Artificial earthquake record used for training of neuro-controller

5. Sensitivity Evaluation

In updating the weights of neural network, response sensitivity to control signal is required in Eq. (5). In the discrete time domain with a zero-order approximation, the sensitivity can be expressed as follows

$$\left\{\frac{\partial y_{k+1}}{\partial u_k}\right\} = \left(e^{AT_s - I}\right)A^{-1}B \tag{10}$$

where T_s is sampling time step (Kim et al. 2000). Although the sensitivity matrix has the mathematical form, it can be easily found by unit impulse test by assuming the system matrices A and B are unknown. When the sampling step is 0.005 s, the sensitivity of the base-isolated structure can be found as Table 1.

Table 1. Numerical results under El Centro earthquake

Direction	$\partial a_8 / \partial y$	$\partial a_b / \partial y$	$\partial d_b / \partial y$
x	-3.50×10^{-4}	-4.78×10^{-1}	-1.90×10^{-6}
y	-5.40×10^{-4}	-4.80×10^{-1}	-2.61×10^{-6}

6. Performance Evaluation

To design a neuro-controller, it is important to decide the structure of neural network. Because the superstructure and the base of the benchmark building are modeled using three master degrees of freedom (DOF) per floor at the center of mass, two neuro-controllers are employed for x and y-directions, respectively. Each neuro-controller has three layers: input layer, hidden layer and output layer. The input layer has five nodes; each node is connected to a feedback signal (building response) that are available for direct measurement. Building responses that can be directly measured include the absolute accelerations at the center of mass of all floor levels and the base, the absolute accelerations and displacements at all device locations, and ground

accelerations. For the controller design reported herein, feedback signals of neuro-controllers at each translational direction consist of base displacement and acceleration, ground excitation, acceleration at the eighth floor, and acceleration at the device location which has the largest acceleration among eight con trol devices under uncontrolled case. The hidden layer has eight nodes and the output layer has only one node that generates desired control force. Moreover, the sigmoid function is used as the activation function for the hidden layer and the linear function is employed for the output layer.

For the cost function, eighth floor acceleration, base acceleration and displacement are included. This is because the evaluation criteria J_1, J_2, J_5, J_8 are directly related with the accelerations of the eighth floor and base, and J_3, J_7 are also related with the base displacement. After trial and error, the optimal weighting matrices was chosen as:

$$\boldsymbol{Q} = \boldsymbol{diag}(0.1, 0.1, 0.001), \quad r = 10^{-15} \tag{11}$$

Moreover, sensor gains for accelerometers are (10/9.81) V/(m/sec2), gain for displacement sensors are 10 V/m, and the load cell sensor gains are (10/2200) V/kN. The sensor measurements are assumed to have identically distributed RMS noise of 0.14 V and are modeled as Gaussian rectangular pulse processes with a pulse width of 0.005 seconds.

The results of the evaluations for the proposed semi-active neuro-controller with linear elastomeric isolation system are presented in Tables 2 and 3 along with their comparisons with those of passive and sample controller results provided by Nagarajaiah and Narasimhan (2005). The results were obtained for the fault normal (FN) component and the fault parallel (FP) acting in two perpendicular directions and were evaluated in terms of the performance indices defined in the base-isolated benchmark paper (Narasimhan et al. 2005). The semi-active force is applied to the base of the structure by sixteen MR dampers, eight in the x-direction and eight in the y-direction. Figure 5 shows the eighth floor time history response under the FP and FN components Sylmar earthquake which are acting on the x and y-axis of the benchmark building.

As shown in Tables 2 and 3, the proposed neuro-control scheme significantly reduces the floor acceleration. However, this is at the cost of slight increase of the base displacement. Note that, under Jiji and Ranadi earthquakes, the peak floor accelerations (J_5) and peak base and floor shear (J_1 and J_2) were worse than the passive control. This is caused by some local peaks of the acceleration. However, if one looks at the RMS floor acceleration (J_8), the proposed controller still performs better than the passive control and has further improvement over the sample controller in some cases.

The corner drift results are provided in Table 4. For all cases except for the FN-X subject to the Jiji earthquake, the proposed neuro-controller demonstrates better performance than that of passive control and sample controller. For the Newhall, El Centro and Kobe earthquake, the corner drifts of passive and sample controller are worse than the uncontrolled case. However, the proposed controller still exhibits better performance comparing with the uncontrolled structure.

7. Conclusion

In this paper, a new semiactive control strategy for seismic response reduction using

neuro-controller and MR dampers is proposed. The proposed control system adopts a training algorithm based on a cost function and sensitivity evaluation algorithm to calculate the desired control force. With this new training algorithm, one does not need to preset the desire structural response and the required effort to train the emulator neural network can be eliminated. A clipped algorithm is then employed to induce the MR damper to generate approximately the desired control force by selecting appropriate command voltage. The proposed semi-active neuro-controller was applied to a benchmark building installed with linear elastomeric isolation system. Comparing with that of passive and sample controller, numerical simulation results have shown that the proposed scheme can significantly reduce the floor accleration, base shear and building corner drift with only a slight increase of the base displacement.

ACKNOWLEDGMENT

The writers gratefully acknowledge the partial support of this research by the Construction Core Technology Research and Development Project (Grant No. C105A1000021) supported by the Ministry of Construction and Transportation and the Smart Infra-Structure Technology Center (SISTeC) supported by the Korea Science Foundation and the Ministry of Science and Technology in Korea.

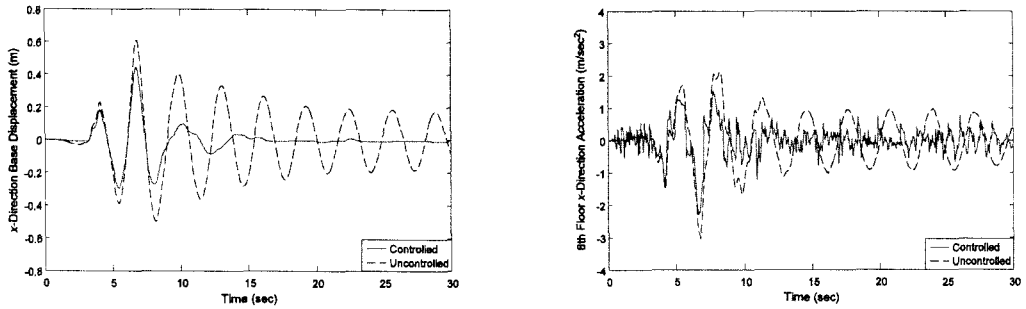

Fig. 5. Performance of the neuro-controller under Sylmar earthquake (FP-X, FN-Y)

Table 2. Results of neuro-controller for linear isolation system (FP-X, FN-Y)

	Newhall			Sylmar			El Centro			Rinaldi			Kobe			Jiji			Erzinkan		
	Pas.	Clip.	Pro.	Pas.	Clip.	Pro.	Pas.	Clip.	Pro.	Pas.	Clip.	Pro.	Pas.	Clip.	Pro.	Pas.	Clip.	Pro.	Pas.	Clip.	Pro.
J_1	0.91	0.97	0.91	0.90	0.90	0.83	0.73	1.25	0.74	0.95	1.05	0.93	0.84	1.04	0.70	0.83	0.84	0.90	0.94	0.93	0.84
J_2	0.95	1.02	0.91	0.92	0.91	0.85	0.87	1.23	0.74	0.96	1.02	0.93	0.81	1.03	0.72	0.82	0.84	0.90	0.95	0.93	0.85
J_3	0.51	0.56	0.72	0.66	0.73	0.76	0.14	0.54	0.36	0.50	0.60	0.65	0.36	0.52	0.46	0.65	0.65	0.80	0.49	0.47	0.56
J_4	1.30	1.04	0.86	0.81	0.87	0.75	1.22	1.26	0.66	0.97	0.97	0.92	1.19	0.99	0.72	0.86	0.86	0.92	0.85	0.86	0.72
J_5	2.49	1.49	1.14	1.49	1.16	0.87	2.85	1.61	1.55	1.12	1.03	1.41	2.34	1.63	1.58	0.92	0.87	0.95	1.21	1.23	0.88
J_6	0.34	0.30	0.30	0.25	0.24	0.24	0.67	0.38	0.53	0.29	0.27	0.26	0.39	0.28	0.37	0.17	0.17	0.16	0.26	0.25	0.25
J_7	0.25	0.33	0.45	0.40	0.45	0.55	0.09	0.41	0.22	0.27	0.38	0.42	0.16	0.26	0.34	0.42	0.46	0.57	0.32	0.34	0.47
J_8	1.07	0.89	0.73	0.82	0.74	0.67	1.61	0.76	0.70	0.83	0.72	0.61	1.14	0.73	0.57	0.82	0.72	0.75	0.60	0.63	0.54
J_9	0.89	0.79	0.75	0.86	0.81	0.72	0.82	0.65	0.82	0.86	0.77	0.71	0.87	0.73	0.74	0.70	0.64	0.55	0.87	0.80	0.71

* Pas. : Passive, Clip. : Clipped optimal, Pro. : Proposed

Table 3. Results of neuro-controller for linear isolation system (FN-X, FP-Y)

	Newhall			Sylmar			El Centro			Rinaldi			Kobe			Jiji			Erzinkan		
	Pas.	Clip.	Pro.	Pas.	Clip.	Pro.	Pas.	Clip.	Pro.	Pas.	Clip.	Pro.	Pas.	Clip.	Pro.	Pas.	Clip.	Pro.	Pas.	Clip.	Pro.
J_1	0.83	0.88	0.80	0.79	0.81	0.72	0.73	1.26	0.78	0.88	0.98	0.84	0.96	1.15	0.91	0.74	0.74	0.82	0.85	0.85	0.76
J_2	0.92	0.92	0.82	0.78	0.79	0.74	0.93	1.25	0.78	0.93	1.01	0.90	1.00	1.20	0.91	0.74	0.73	0.81	0.85	0.84	0.76
J_3	0.51	0.55	0.65	0.68	0.74	0.75	0.19	0.65	0.54	0.53	0.62	0.64	0.40	0.53	0.51	0.63	0.63	0.77	0.51	0.51	0.56
J_4	1.32	1.24	0.82	0.80	0.79	0.80	2.18	1.41	0.97	0.93	0.99	0.96	1.30	1.33	0.99	0.74	0.73	0.78	0.95	0.88	0.77
J_5	1.86	1.40	1.16	1.25	0.92	0.84	3.46	1.93	1.99	1.12	1.02	0.98	2.24	1.48	1.27	0.77	0.80	0.80	1.13	1.16	0.82
J_6	0.34	0.30	0.33	0.25	0.23	0.25	0.69	0.37	0.51	0.28	0.26	0.26	0.41	0.30	0.37	0.71	0.17	0.14	0.25	0.24	0.25
J_7	0.33	0.42	0.55	0.46	0.51	0.55	0.12	0.45	0.29	0.24	0.30	0.39	0.20	0.38	0.37	0.40	0.46	0.59	0.29	0.32	0.42
J_8	1.05	0.84	0.73	0.67	0.61	0.54	1.99	0.92	0.94	0.58	0.47	0.43	1.44	0.98	0.88	0.74	0.61	0.68	0.48	0.52	0.46
J_9	0.88	0.79	0.75	0.85	0.81	0.70	0.81	0.70	0.82	0.87	0.78	0.71	0.87	0.71	0.74	0.70	0.64	0.53	0.87	0.78	0.73

* Pas. : Passive, Clip. : Clipped optimal, Pro. : Proposed

Table 4. Results for corner drifts normalized by uncontrolled values

	Passive		Clipped Optimal		Proposed	
	FP-X	FN-X	FP-X	FN-X	FP-X	FN-X
Newhall	1.50	1.21	1.28	1.11	1.01	0.74
Sylmar	0.76	0.86	0.96	0.90	0.75	0.71
El Centro	1.10	2.06	0.93	1.30	0.57	0.91
Rinaldi	0.91	0.89	0.89	0.93	0.84	0.94
Kobe	1.22	1.06	1.07	1.10	0.80	0.85
Jiji	0.80	0.96	0.78	0.92	0.77	1.01
Erzinkan	0.72	0.90	0.73	0.94	0.65	0.74

REFERENCE

1. Chen, H. M., Tsai, K. H., Qi, G. Z., Yang, J. C. S., and Amini, F. "Neural network for structural control." *Journal of Computing in Civil Engineering*, Vol. 9, No. 2, 1995, pp.168–176.
2. Ghaboussi, J., and Joghataie, A. "Active control of structure using neural networks." *Journal of Engineering Mechanics*, Vol. 121, No. 4, 1995, pp. 555–567.
3. Kim, J. T., Jung, H. J., and Lee, I. W. "Optimal structural control using neural networks." *J. Eng. Mech.*, Vol. 126, No. 2, 2000, pp. 201–205.
4. Kim, D. H., and Lee, I. W. "Neuro-control of seismically excited steel structure through sensitivity evaluation scheme." *Earthquake Engineering andStructural Dynamics*, Vol. 30, No. 9, 2001, pp. 1361–1378.
5. Lee, H. J., Jung, H. J., Thanh, N. X., Park, S. K., Lee, I. W. "Semiactive neuro-control for seismically excited structure using MR damper." *Proc. of 9th East Asia-Pacific Conf. on Structural Engineering and Construction*, Bali, Indonesia; 2003, CD-ROM
6. Narasimhan S., Nagarajaiah S., Johnson E. A. and Gavin H. P. "Smart base isolated benchmark building part I: Problem definition." *Journal of Structural Control and Health Monitoring* in print